Eur Biophys J (1986) 13: 331–342

European Biophysics Journal

Conformational dynamics of the anticodon loop in yeast $tRNA^{Phe}$ as sensed by the fluorescence of wybutine

F. Claesens and R. Rigler*

Department of Medical Biophysics, Karolinska Institute, Box 6 04 00, S-10401 Stockholm, Sweden

Received May 28, 1985/Accepted in revised form December 9, 1985

Abstract. Conformational and dynamic properties of the anticodon loop of yeast $tRNA^{Phe}$ were investigated by analyzing the time resolved fluorescence of wybutine serving as a local structural probe adjacent to the anticodon GmAA on its 3′ side. The influence of Mg^{2+}, important for stabilizing the tertiary structure of tRNA, and of the complementary anticodon s^2UUC of *E. coli* $tRNA_2^{Glu}$ were investigated.

Fluorescence lifetimes and anisotropies were measured with ps time resolution using time correlated single photon counting and a mode locked synchronously pumped and frequency doubled dye laser as excitation source. From the analysis of lifetimes (τ) and rotational relaxation times (τ_R) we conclude that wybutine occurs in various structural states: *(i)* one stacked conformation where the base has no free mobility and the only rotational motion reflects the mobility of the whole tRNA molecule ($\tau = 6$ ns, $\tau_R = 19$ ns), *(ii)* an unstacked conformation where the base can freely rotate ($\tau = 100$ ps, $\tau_R = 370$ ps) and *(iii)* an intermediary state ($\tau = 2$ ns, $\tau_R = 1.6$ ns).

Under biological conditions, i.e. in the presence of Mg^{2+} and neutral salts, wybutine is found in a stacked and immobile state which is consistent with the crystallographic picture. In the presence of the complementary codon however, as exemplified by the *E. coli*-$tRNA_2^{Glu}$ anticodon, our analysis indicates that the codon-anticodon complex exists in an equilibrium of structural states with different rotational mobility of wybutine. The conformation with wybutine freely mobile is the predominant one and suggests that this conformation of the codon-anticodon structure differs from the canonical 3′–5′ stack.

Key words: Picosecond fluorescence spectroscopy, transfer-RNA, wybutine, dynamics

* To whom offprint requests should be sent

Introduction

tRNA plays an important role in protein synthesis by translating the genetic code into a peptide sequence. Several models proposed for describing the mechanism of protein synthesis involve the anticodon loop flipping between a (5′–3′)- and a (3′–5′)-stacked conformation (Woese 1970; Lake 1977). It has been suggested that even overall changes in the tRNA can take place, for example when passing the polypeptide chain from one tRNA to another. Until now mainly X-ray crystallographic studies have provided information on the structure of tRNA (Kim et al. 1974; Ladner et al. 1975), and it was found that the structure of the anticodon loop is best described by a 3′–5′ stacked conformation. This conformation, however, represents a time and space average of a structure which is characterized by a high temperature factor (Quigley and Rich 1982).

Recently attempts have also been made to obtain information about the solution structure of tRNA, especially about the anticodon loop of yeast $tRNA^{Phe}$ by nuclear magnetic resonance measurements (NMR) (Geerdes et al. 1980a, b; Clore et al. 1984). Geerdes et al. (1980a, b) studied the effect of codon-anticodon interaction by binding UUC, UUCG, UUCA and UUCAG to yeast $tRNA^{Phe}$ and monitoring the ^1H and ^{31}P spectra. They could show that in the case of UUCAG, the anticodon loop adopts a 5′–3′ stack. Clore et al. (1984) studied the structure of the anticodon loop and stem region of $tRNA^{Phe}$ with and without the codon UUC present by time resolved nuclear Overhauser enhancement measurements and found that in both cases the anticodon loop adopted the 3′–5′ stacked conformation.

In order to shed additional light on conformations and dynamics of the anticodon structure in solution we have studied the fluorescence of the hypermodified nucleotide wybutine *Y* (Eisinger et al. 1970) which is situated at position 37 adjacent

to the 3′ side of the anticodon G_mAA and serves as structural probe.

Recent advances in time resolved fluorescence spectroscopy (Rigler et al. 1984) permit a time resolution of a few ps and thus the detection of very short lived fluorescence states as well as fast rotational motions.

Mg^{2+} ions are known to have a stabilizing effect on the three-dimensional folding of tRNA's and are important for their biological function. For this reason the influence of Mg^{2+} on the fluorescence properties and rotational motion of wybutine was examined as well as the effect of binding a complementary codon to the anticodon of yeast $tRNA^{Phe}$. As a "codon", the anticodon s^2UUC of *E. coli* $tRNA_2^{Glu}$ was used, because it has a high binding constant to yeast $tRNA^{Phe}$ as compared to the trinucleotide UUC (Eisinger 1971; Yoon et al. 1975). It has also been argued that the interaction between two tRNA loops might reflect the evolutionary origin of the genetic code and that on the ribosome the mRNA may fold into a loop itself (Grosjean et al. 1978). In this study the single photon counting method was applied and the fluorescence lifetimes of the wybutine as well as its rotational motion were measured. It was found that in the presence of Mg^{2+} wybutine in the yeast $tRNA^{Phe}$ molecule has a major long fluorescence lifetime and is in a fixed conformation, but it has a short fluorescence lifetime and becomes mobile when the yeast $tRNA^{Phe}$-*E. coli*-$tRNA_2^{Glu}$ complex is formed.

Experimental

Materials

Yeast $tRNA^{Phe}$ (lot 1190326) and *E. coli* $tRNA_2^{Glu}$ (lot 1402109) were from Boehringer Mannheim. Their amino acid acceptance was tested and found to be 1,400 pmoles/unit OD_{260} and 1,300 pmoles/unit OD_{260} respectively, which is in accordance with the values specified by the manufacturer. Both tRNA's were run on a polyacrylamide gel to test their purity. The tRNA's were dialyzed three times at 4 °C against 3 changes of a buffer containing 10 m*M Tris*, 0.1 *M* KCl, 0.1 m*M* EDTA, pH 7.5. During the measurements the same buffer was used to which 0.1 m*M* DTT and $MgCl_2$, from 0.02 m*M* to 20 m*M*, were added. Before each measurement the sample was warmed up to 65 °C for about 5 min to allow the tRNA's to adopt their native conformations. In calculating tRNA concentrations a factor of 1.6 μ*M*/unit OD_{260} was used. Ethidium bromide (EB) was a gift of Boots Pure Drug Co. Ltd. (Nottingham) and 1 : 1 tRNA : EB complexes were prepared.

Method

Time resolved measurements of the wybutine fluorescence were carried out using time correlated single photon counting in an improved instrument (Rigler et al. 1985) originally described previously (Rigler and Ehrenberg 1976). The system estimates variations in intensity and timing of the exciting pulse as well as of the fluorescence response. As an excitation source a mode-locked CR 3000K Coherent Krypton ion laser was used, pumping synchronously a Rhodamine 6G dye laser, and generating 6 ps pulses with 76 MHz repetition rate. In order to increase the peak power of the individual pulses and to match the repetition rate to the time to amplitude converter (TAC) of the single photon detection system the output of the dye laser was cavity dumped. The emitted beam had a wavelength of 600 nm and was frequency doubled in an angular tuned KDP crystal so that the resulting beam had a wavelength of 300 nm. In order for the final polarization to be vertical a half wavelength plate was placed before the KDP crystal which turned the polarization of the 600 nm beam into a horizontal one. The emitted frequency doubled beam was then vertically polarized. For detection a Hamamatsu multichannel plate R1564U was used after a KV418 cut-off filter. The photoelectron pulses were amplified in a high bandwidth preamplifier (EG&G, ESN VT 110). Start and stop (from a reference diode, HP 2-4220) signals for the TAC (Ortec 457) were discriminated in Ortec 583 and Tenelec 453 constant fraction discriminators. The FWHM of the frequency doubled laser pulse as detected by the system was 43 ps (Rigler et al. 1984).

Data evaluation

In the fluorescence decay measurements the excitation pulse, the unpolarized fluorescence (with the analyzer under the magic angle), the fluorescence polarized parallel with the exciting beam and the dark current were measured sequentially during several cycles and stored in 4 groups, 2048 channels each, in a Nuclear Data ND66 multichannel analyzer. For most experiments the time interval per channel was 21.4 ps which resulted in a total time scale of 44 ns for each group. The excitation pulse was detected at 300 nm using a beam splitter and recorded for carrying out the convolution of system response and decay models (see below). Here use was made of the wavelength independent response of the proximity type microchannel plate (R1564U) (Rigler et al. 1985). Since a lens system and cut-off filters were used in the fluorescence detection pathway there was a difference in optical pathlength between the excitation and fluorescence beam, which

was taken care of by introducing a constant and experimentally determined time shift in the data evaluation.

In the data analysis physical models, describing the decay of unpolarized and parallel polarized fluoressence, were convoluted with the measured excitation pulse using the algorithm of Grinvald and Steinberg (1974). These functions and their parameters were compared with the experimentally measured decays using a program for non linear regression (Meeter 1964) based on an algorithm of Marquardt (1963). The minimization was modified so that maximum likelihood estimates of the parameters were obtained (Rigler and Ehrenberg 1976). The X^2 values given are defined according to

$$X^2 = 1/(N-C)\sum_{i=1}^{N}(e_i - f_i)^2/f_i\,, \tag{1}$$

e_i is the measured emission intensity averaged in channel i, and f_i is its theoretically predicted value. C is the number of parameters and N is the number of observables. The sum of squares is a X^2-distributed stochastic variable with expectation value 1 and $N-C$ degrees of freedom. When the statistics of a data set as such were considered to be insufficient to fit a certain model, as is the case for rotational times, several experiments were evaluated together. This was done by joint evaluation of the data of different experiments in one vector and minimization of all points simultaneously to the calculated values of the model (Ehrenberg et al. 1979). The rotational times in this case were the same for every experiment while the anisotropy amplitudes were fitted for each data set separately.

Fluorescence lifetimes

The unpolarized fluorescence $I_m(t)$ is described by a sum of discrete fluorescence lifetimes which decay exponentially, according to the model

$$I_m(t) = \sum_i a_i \exp(-t/\tau_i)\,, \tag{2}$$

where τ_i are the different fluorescence lifetimes and a_i their respective amplitudes. The amplitude a_i is proportional to $\varepsilon_i(\lambda)\, k_i(\lambda)\, c_i$ where $\varepsilon_i(\lambda)$ is the absorption coefficient, $k_i(\lambda)$ the radiative rate constant and c_i is the fraction of molecules that exists in state i.

Fluorescence anisotropy

The decay of the fluorescence anisotropy $r(t)$ was calculated directly from the measured unpolarized $I_m(t)$ and parallel polarized $I_{ll}(t)$ fluorescence components. $r(t)$ was obtained from the ratio of $I_{ll}(t)$ and $I_m(t)$ (Rigler and Ehrenberg 1976).

$$r(t) = (I_{ll}(t)/I_m(t) - 1)/2\,. \tag{3}$$

Because of the short response time of the detection system the anisotropy decay can be evaluated directly from the measured curves without the use of models and deconvolution procedures.

Rotational relaxation times

Since the anisotropy is a complicated function of both rotational relaxation times and fluorescence decay times (Rigler and Ehrenberg 1973; Cross et al. 1983; Szabo 1984), rotational relaxation times τ_R cannot, in general, be evaluated immediately from these curves. For that reason numerical calculations were performed according to two models.

The first model describes the rotation of a sphere which has several fluorescence lifetimes and the anisotropy amplitude r_0, as well as τ_R, are obtained from:

$$I_{ll}(t)/I_m(t) = (1 + 2r_0)\exp(-t/\tau_R) \tag{4}$$

with $1/\tau_R = 6D_R$ where D_R is the rotational diffusion constant.

In the second model rotational times are fitted for different rotors each specified by its own lifetime.

$$I_{ll}(t)/I_m(t) = \sum_i (1 + 2r_{0i})\exp(-t/\tau_{Ri})\, a_i \exp(-t/\tau_i)/\sum_i a_i \exp(-t/\tau_i)\,. \tag{5}$$

Substituting the fluorescence lifetimes and amplitudes calculated from the unpolarized fluorescence one obtains the rotational relaxation times, τ_R, and their anisotropy amplitudes r_0. For parametrization of the given model convolution of the model with the laser pulse was carried out. In order to compensate for differences in detection sensitivity between the magic angle and the parallel position a correction factor was introduced. This correction factor was determined experimentally by exciting ethidium bromide by a laser pulse which was polarized perpendicularly to the direction normally used. The fluorescence decay for the I_m and I_{ll} directions were measured and the ratio of the integrated decay curves was calculated to give a correction factor of 0.91.

Time resolved fluorescence spectra

Time resolved fluorescence spectra of the wybutine were recorded for different time windows set by the discriminators in the analog to digital converter (ADC) of the ND66 when run in the pulse height

analysis mode (PHA). For measuring the fluorescence spectra the multichannel scaling mode (MCS) was used. In the detection system a Zeiss M_4QIII prism monochromator was used with a bandwidth of about 20 nm. The excitation wavelength was 300 nm as in the fluorescence decay measurements. A time spread of 10 ps at 340 nm was calculated from the dispersion data.

Fluorescence titrations

In order to determine the binding constant, K, for the formation of the yeast $tRNA^{Phe}$-*E. coli* $tRNA_2^{Glu}$ complex fluorescence titrations, in which the stationary fluorescence was measured, were carried out. The excitation source was a Xe 200 W high pressure lamp and the excitation wavelength, 300 nm, was selected by a Zeiss M_4QIII monochromator. The fluorescence was detected by a SSR Quantum Photometer after a KV418 filter. The yeast $tRNA^{Phe}$ concentration of 0.5 μM was kept constant while *E. coli* $tRNA_2^{Glu}$ was added. The data were evaluated according to Benesi and Hildebrand (1949) from the graph:

$$1/v = 1 + 1/c_B K \tag{6}$$

where v is the fraction of bound tRNA, c_B is the amount free *E. coli* $tRNA_2^{Glu}$ and K is the binding constant. It was assumed that upon saturation the quenching of the fluorescence is complete.

Anisotropy amplitude

In order to obtain information about the orientation of the absorption and emission dipole moments relative to each other the limiting anisotropy value at $t = 0$ was determined for the wybutine in yeast $tRNA^{Phe}$. The motion of the tRNA molecule and of the wybutine itself was reduced by using a solution containing 65% glycerol as solvent. The steady state anisotropy was measured in the same instrument as described for fluorescence titrations, except that a polarizer before and an analyzer after the sample were added so that the fluorescence polarized parallel and perpendicular to the excitation beam could be detected. Measurements were carried out at different temperatures and the limiting anisotropy at $t = 0$ was deduced from Perrin plots according to

$$1/A = (1/A_0)\,(1 + \tau_F\, kT/V_h\, \eta) \tag{7}$$

by extrapolation to $T/\eta = 0$.

Table 1. Equilibrium constants K for yeast $tRNA^{Phe}$ interacting with *E. coli* $tRNA_2^{Glu}$ at various concentrations of Mg^{2+} and different temperatures

Mg^{2+} concentration in mM	T [°C]	$K \cdot 10^{-6}$ [M^{-1}]
20	20	1.2
20	12	2.9
20	4	6.7
0.1	4	0.35
1	4	0.76
20	4	6.7

Results

Equilibrium binding constants

The binding constant, K, for the formation of the yeast $tRNA^{Phe}$-*E. coli* $tRNA_2^{Glu}$ complex was determined from fluorescence titrations under stationary excitation for different Mg^{2+} concentrations and at different temperatures (Table 1). The errors were estimated to be 30% or less. It can be noticed that the binding constant is sensitive to temperature and in particular to the concentration of Mg^{2+} ions. While K increases by about a factor of five when the temperature is decreased from 20° to 4 °C, it increases by a factor of twenty when the Mg^{2+} concentration is raised from 0.1 to 20 mM.

The change in enthalpy and entropy derived from the temperature dependence of these constants are $\Delta H = -17 \pm 3$ kcal/mole and $\Delta S = -30 \pm 10$ cal/°mole. The values are in agreement with those found in the literature (Eisinger 1971; Grosjean et al. 1976).

Fluorescence lifetimes of wybutine

The influence of magnesium ions. First the influence of Mg^{2+} ions on the fluorescence properties of the wybutine in the yeast $tRNA^{Phe}$ molecule was investigated. The yeast $tRNA^{Phe}$ concentration was 2.7 μM and the Mg^{2+} concentration varied from 0.02 to 20 mM. The decay curve of the first and last point at 20 °C are shown (Fig. 1A, B). At least three fluorescence lifetimes τ_i were needed to describe the fluorescence decay, each of which is considered to be specific for a certain environment of the wybutine.

Table 2. Excited state lifetimes τ_i of wybutine in yeast $tRNA^{Phe}$ at various concentrations of Mg^{2+} at 20 °C

mM Mg^{2+}	τ_1 [ns]	τ_2 [ns]	τ_3 [ns]	χ^2
0.02	0.34 ± 0.01	2.34 ± 0.03	5.18 ± 0.03	1.44
1	0.23 ± 0.02	2.72 ± 0.07	6.33 ± 0.02	1.23
2	0.23 ± 0.03	2.7 ± 0.1	6.34 ± 0.02	1.24
5	0.23 ± 0.03	2.9 ± 0.2	6.36 ± 0.02	1.30
10	0.21 ± 0.03	2.8 ± 0.2	6.34 ± 0.02	1.25
20	0.21 ± 0.04	2.8 ± 0.4	6.25 ± 0.02	1.33

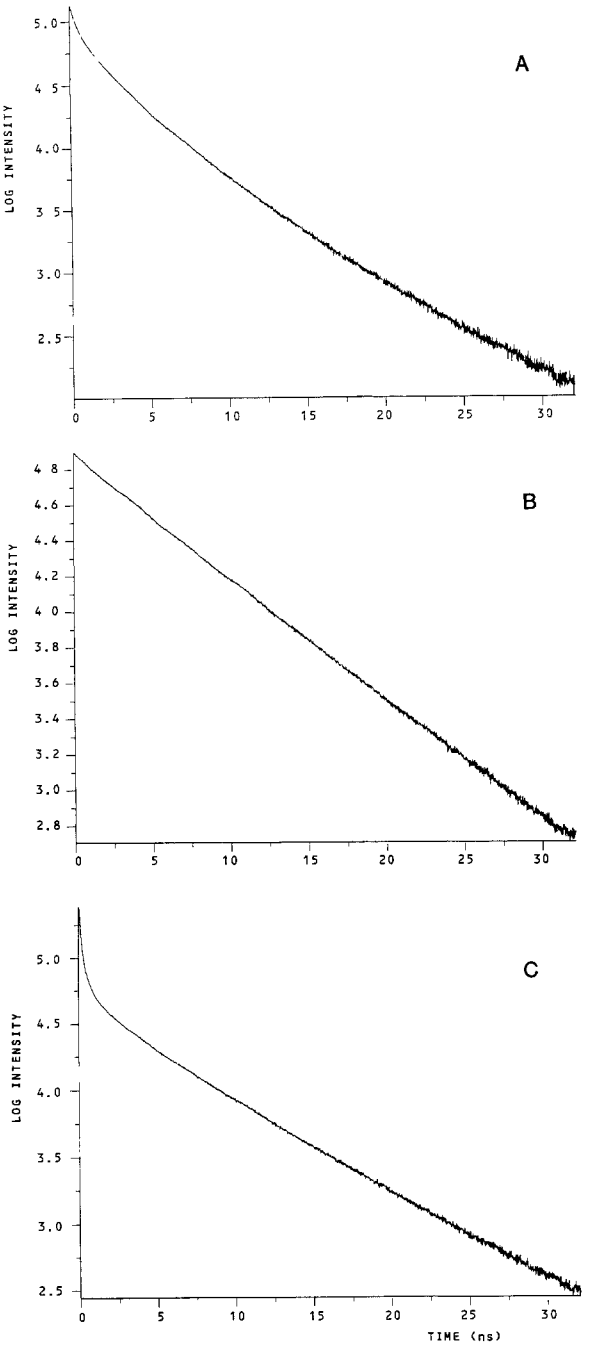

Fig. 1 A–C. Fluorescence decay of wybutine in yeast $tRNA^{Phe}$ at 0.02 m*M* Mg^{2+} (**A**), 20 m*M* Mg^{2+} (**B**) and in the yeast $tRNA^{Phe}$-*E. coli* $tRNA_2^{Glu}$ complex at 20 m*M* Mg^{2+} (**C**)

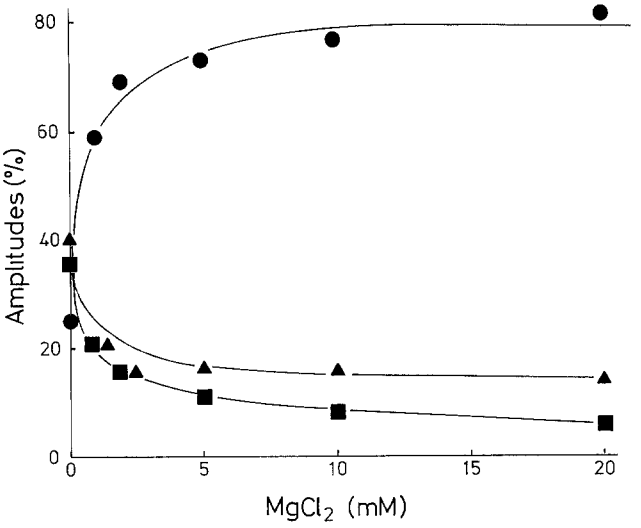

Fig. 2. Distribution of the relative amplitudes a_1 (▲), a_2 (■) and a_3 (●) of the fluorescence lifetimes of wybutine in yeast $tRNA^{Phe}$ as a function of Mg^{2+} concentration at 20 °C

They are given in Table 2. The shortest lifetimes, τ_1, decreases slightly as a function of the Mg^{2+} concentration from 0.34 to 0.21 ns. The two longest lifetimes, τ_2 and τ_3, roughly 3 ns and 6 ns respectively, were constant throughout the Mg^{2+} series, except for the lowest concentration. A similar behaviour of the Mg^{2+} concentration dependence of the lifetimes was found previously for ethidium labeled yeast $tRNA^{Phe}$ (Ehrenberg et al. 1979) and could be attributed to different accessibility of ethidium to quenching ions. A plot of the distribution of the relative amplitudes, a_i, is shown in Fig. 2.

Assuming that the spectroscopic constants (ε_i, k_i) do not change for the wybutine at different Mg^{2+} concentrations these a_i directly reflect the percentage of wybutines that can be found in state *i*. At 0.02 m*M* Mg^{2+} these three states are nearly equally populated. At 20 m*M* Mg^{2+} however most of the wybutines (80%) are in the long lifetime state (6 ns) while the remaining 20% are divided between the two states with the shorter lifetimes.

The influence of the E. coli $tRNA_2^{Glu}$ anticodon: Fluorescence lifetimes of the wybutine in the yeast $tRNA^{Phe}$-*E. coli* $tRNA_2^{Glu}$ complex were also measured for different concentrations of equimolar mixtures of the two tRNA's at 20 m*M* Mg^{2+} and at three different temperatures, 4°, 12° and 20 °C. A decay curve for a concentration of 30 μ*M* for each tRNA at 20 °C is shown (Fig. 1 C), which means that about 85% of the complex is formed. Here too, the unpolarized decay curves were fitted with three fluorescence lifetimes, τ_i, and amplitudes, a_i. Table 3 lists the lifetimes at 20 °C. It is apparent that upon complex formation a very short lifetime of the wybutine becomes prominent, compared to the lifetime distribution of the wybutine in the yeast $tRNA^{Phe}$ molecule alone. The three lifetimes fitted are now approximately 0.1, 1 and 6 ns. A higher saturation of binding leads to a higher population of the 100 ps state. A plot of the distribution of the relative amplitudes for the three temperatures is given in Fig. 3. From this it becomes clear that a

Table 3. Excited state lifetimes τ_i of wybutine in yeast $tRNA^{Phe}$ at various degrees of saturation with *E. coli* $tRNA_2^{Glu}$ at 20 m*M* Mg^{2+} and 20 °C

Concentration of yeast $tRNA^{Phe}$ and *E. coli* $tRNA_2^{Glu}$ (equimolar mixture) in μm	Fractional saturation of yeast $tRNA^{Phe}$ [%]	τ_1 [ns]	τ_2 [ns]	τ_3 [ns]	χ^2
1.25	33	0.123 ± 0.004	1.99 ± 0.08	6.27 ± 0.01	1.24
2.5	45	0.119 ± 0.003	2.21 ± 0.09	6.22 ± 0.01	1.43
5	57	0.107 ± 0.002	1.60 ± 0.05	6.18 ± 0.01	1.44
10	67	0.105 ± 0.002	1.27 ± 0.03	6.06 ± 0.01	1.33
20	75	0.103 ± 0.002	1.19 ± 0.03	5.98 ± 0.01	1.48
40	82	0.105 ± 0.002	1.14 ± 0.03	5.96 ± 0.01	1.51
60	85	0.100 ± 0.002	1.02 ± 0.02	5.94 ± 0.01	1.57

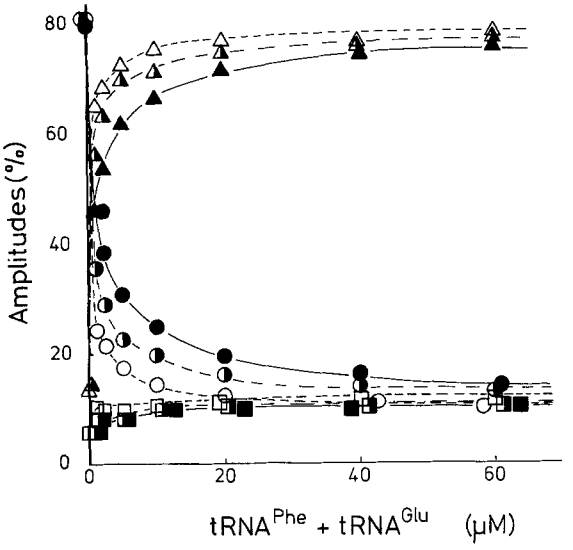

Fig. 3. Distribution of the relative amplitudes a_1 (▲, ◮, △), a_2 (■, ◨, □) and a_3 (●, ◑, ○) of the fluorescence lifetimes of wybutine in the yeast $tRNA^{Phe}$-*E. coli* $tRNA_2^{Glu}$ complex at 20 m*M* Mg^{2+} as a function of tRNA concentration. The curves are shown for 20 °C (▲, ■, ●), 12 °C (◮, ◨, ◑) and 4 °C (△, □, ○)

lower temperature enhances the binding and thus populates the shortest lifetime state more than the higher temperatures. The longest lifetime, 6 ns, can be interpreted as representing the amount of unbound yeast $tRNA^{Phe}$, according to its relative amplitude. A change in temperature only leads to a change of the longest lifetime and not of the shorter ones. At 12 °C τ_3 is about 7.5 ns and at 4 °C τ_3 has the value of 8.5 ns. One can thus conclude that upon complex formation a change in the environment of the wybutine takes place which leads to a completely different distribution of the fluorescence lifetimes in which a conformation of the wybutine specified by a very short lifetime of 100 ps is the main feature.

Anisotropy decay

Anisotropy curves for the wybutine in the yeast $tRNA^{Phe}$ molecule alone and in the yeast $tRNA^{Phe}$-*E. coli* $tRNA_2^{Glu}$ complex were calculated from the experimental unpolarized and parallel polarized fluorescence decays. They are shown in Fig. 4 for the time range to 3 ns and in Fig. 5 for the time range to 30 ns.

At low Mg^{2+} concentration (0.02 m*M*) the anisotropy curve of yeast $tRNA^{Phe}$ consists of two opposing components and assumes a starting value of 0.03. Statistically the data do not allow one to fit a detailed model, but it is likely that the fastest process, in the time range of 0.5 ns (Fig. 4A), reflects the motion of the wybutine itself and the longer one the rotation of the whole molecule (Fig. 5A). This mobility of the wybutine could explain the short fluorescence lifetimes, since during rotational motion multiple interactions of the wybutine with its environment can lead to a fast non-radiative deactivation of the excited state.

In contrast, at high Mg^{2+} concentration (20 m*M*) wybutine itself is not mobile (Fig. 4B). The only rotation which can be measured is that of the tRNA molecule as a whole (Fig. 5B). The limiting anisotropy value is 0.05 in this case. In the complex of the two tRNA molecules, however, at 20 m*M* Mg^{2+} a very fast depolarization of the fluorescence of wybutine can be noticed (Fig. 4C) which can be explained by a fast rotation of the wybutine itself. This is superimposed on a slow depolarization due to unbound $tRNA^{Phe}$ (Fig. 5C). The rotational time of the complex is too long to be measured with the short lifetimes characteristic for the complex (0.1 and 1 ns). The total anisotropy amplitude has increased to 0.07.

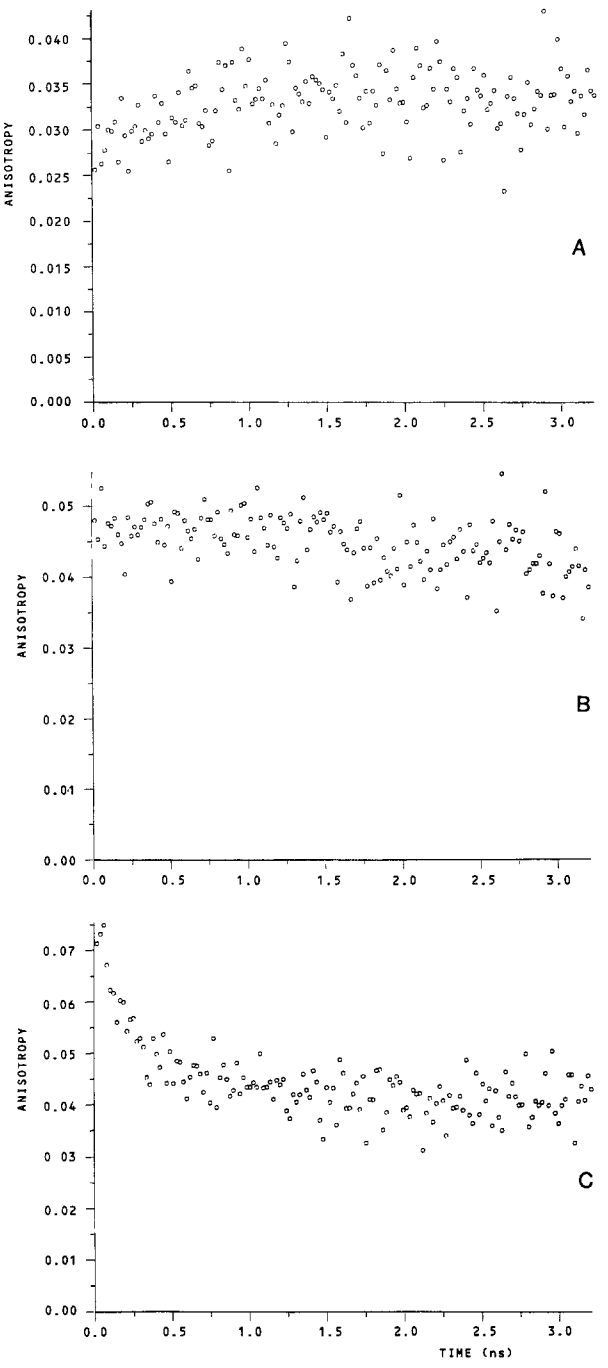

Fig. 4A–C. Fluorescence anisotropy decay for wybutine in yeast $tRNA^{Phe}$ at 0.02 m*M* Mg^{2+} (**A**), 20 m*M* Mg^{2+} (**B**) and in the yeast $tRNA^{Phe}$-*E. coli* $tRNA_2^{Glu}$ complex at 20 m*M* Mg^{2+} (**C**) in a time range up to 3 ns

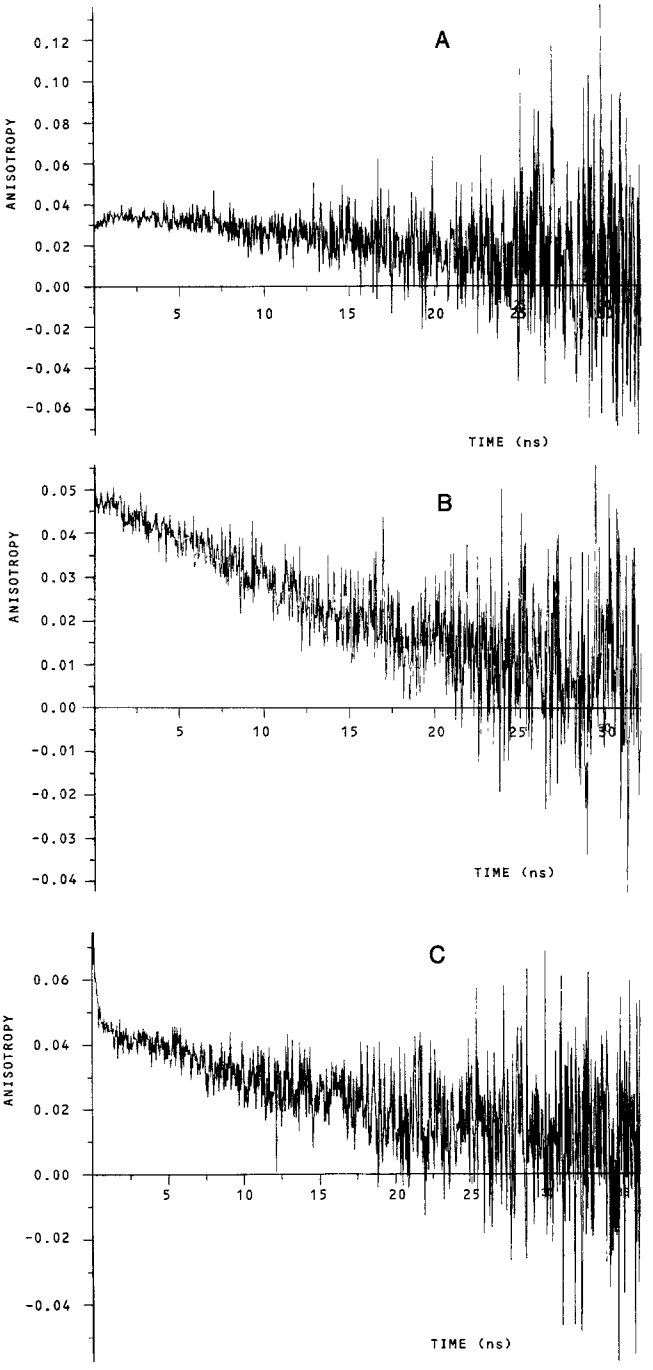

Fig. 5A–C. Fluorescence anisotropy decay for wybutine in yeast $tRNA^{Phe}$ at 0.02 m*M* Mg^{2+} (**A**), 20 m*M* Mg^{2+} (**B**) and in the yeast $tRNA^{Phe}$-*E. coli* $tRNA_2^{Glu}$ complex at 20 m*M* Mg^{2+} (**C**) in a time range up to 30 ns

Rotational relaxation times

The rotational time of the yeast $tRNA^{Phe}$ molecule as seen by the wybutine was determined by using the first model (Eq. (4)), in which the rotational motion of one rotor, having several fluorescence lifetimes, is described. In this case the 20 m*M* Mg^{2+} point was taken and a value of 19 ns for τ_R was obtained at 20 °C. The anisotropy amplitude was 0.05, which is in agreement with measurements of the limiting anisotropy at $t = 0$ by Perrin plots where a value of 0.06 was found for excitation at 300 nm.

The same measurements carried out with ethidium bromide as a fluorescent probe, which

Table 4. Rotational diffusion times τ_{Ri} and anisotropy amplitudes r_i of wybutine in yeast $tRNA^{Phe}$ and in the yeast $tRNA^{Phe}$-*E. coli* $tRNA_2^{Glu}$ complex at 20 m*M* Mg^{2+} and 20 °C

	τ_{R1} [ns]	τ_{R2} [ns]	τ_{R3} [ns]	χ^2
Yeast $tRNA^{Phe}$-*E. coli* $tRNA_2^{Glu}$ complex	0.37 ± 0.06	1.6 ± 0.3	16.2 ± 0.1	1.00
Yeast $tRNA^{Phe}$			19.0 ± 0.1	1.07
Concentration of yeast $tRNA^{Phe}$ and *E. coli* $tRNA_2^{Glu}$ (equimolar mixture) in μ*M*	r_1	r_2	r_3	
5	0.095	0.031	0.056	
10	0.107	0.044	0.060	
20	0.080	0.053	0.050	
60	0.108	0.064	0.052	
Yeast $tRNA^{Phe}$			0.052	

The calculated standard errors for r_1 and r_2 are 0.001 and they are less than that for r_3

Table 5. Rotational diffusion times τ_{Ri} of wybutine in the yeast $tRNA^{Phe}$-*E. coli* $tRNA_2^{Glu}$ complex at 20 m*M* Mg^{2+} and various temperatures

T [°C]	τ_{R1} [ns]	[a]	τ_{R2} [ns]	[a]	τ_{R3} [ns]	[a]	χ^2
20	0.37 ± 0.06	0.37	1.6 ± 0.3	1.6	16.2 ± 0.1	16	1.00
12	0.48 ± 0.09	0.38	2.5 ± 0.4	2.0	21.5 ± 0.3	16	1.02
4	0.6 ± 0.1	0.38	3.3 ± 0.4	2.0	25.6 ± 0.4	17	1.12

[a] are the values obtained for τ_{Ri} after correction for the viscosity effect to 20 °C

binds unspecifically to the tRNA molecule, gave a similar rotational time, τ_R (17.4 ± 0.3 ns), while for the yeast $tRNA^{Phe}$-*E. coli* $tRNA_2^{Glu}$ complex with ethidium bromide a value of 30.0 ± 0.3 ns was obtained for τ_R. In the case of the yeast $tRNA^{Phe}$-*E. coli* $tRNA_2^{Glu}$ complex, it is clear from the anisotropy curve that the fast motion of the wybutine should be taken into account. In the model used now the assembly of tRNA's is considered to consist of three independent configurations. In each conformation wybutine is specified by its own fluorescence lifetime as well as rotational time. In order to improve the data statistics several experiments were evaluated together sharing common τ_{Ri} values. The results are given in Table 4, together with the values obtained for wybutine in the yeast $tRNA^{Phe}$ molecule alone. Assuming that each conformational state of the wybutine has its own rotational motion, one can ascribe a fast rotation with a characteristic time of 370 ps to the state with the shortest lifetime of 100 ps and a motion with a time of 1.6 ns to the 1 ns lifetime state. In the long lifetime state of 6 ns the wybutine itself appears to be immobilized and the rotational time of 16 ns for the yeast $tRNA^{Phe}$ molecule is measured. This supports the idea that the long lifetime only reflects the amount of unbound yeast $tRNA^{Phe}$, which also explains the difference from the results for τ_r when the $tRNA^{Phe}$-$tRNA_2^{Glu}$ complex is labelled by the long lived ethidium bromide. The rotational times were also measured for the highest yeast $tRNA^{Phe}$-*E. coli* $tRNA_2^{Glu}$ concentration of 30 μ*M* at 12° and 4 °C. The results are given in Table 5 showing that all three rotational times scale with T/η and lack significant activation barriers.

The model used is an approximation, since the anisotropy function as such contains terms of both the rotational diffusion of the wybutine and of the complex. Considering the tRNA complex as a sphere to which the wybutine is attached, which can rotate freely around one axis, the anisotropy function is given by (Rigler and Ehrenberg 1973)

$$r(t) = A \exp -(D_w + 6D_c)\, t + B \exp -(4D_w + 6D_c)\, t + C \exp -6D_c t\,, \quad (8)$$

where A, B and C are functions of the angles of the absorption and emission dipole moments relative to the rotational axis and to each other, while D_w is the diffusion constant of the wybutine and D_c that of the

tRNA complex. Carrying out the appropriate approximations one can simplify this model to the one used in our evaluations, while giving the following physical interpretation to the different rotational times.

Shortest rotational relaxation time. In the time range of the shortest fluorescence lifetime (100 ps) the second term of Eq. (8) is dominant:

$$r(t) \approx B \exp(-4 D_w t) + \text{const} \quad \text{with} \quad D_w \gg D_c . \tag{9}$$

This means that the shortest rotational relaxation time is related to $4 D_w$.

Intermediate rotational relaxation time. The intermediate rotational time is found to be about four times longer than the shortest one and can be related to D_w in the first term of Eq. (8). This time cannot be measured with the shortest fluorescence lifetime and thus shows up in the intermediate fluorescence lifetime state.

Long rotational relaxation time. It was mentioned before that the rotation of the whole tRNA complex cannot be measured because of the short fluorescence lifetime specific for the complex. This means that for the long lifetime state only the rotation of the uncomplexed yeast $tRNA^{Phe}$ molecule contributes to the loss of polarization. Thus only the last term in the expression of $r(t)$ is important.

$$r(t) = C \exp -6 D t . \tag{10}$$

The fact that the fluorescence anisotropy decay curve, shown in Fig. 4C, does not decay to zero immediately, but shows residual anisotropy has been interpreted in other situations as due to limited rotation of the emitting species. From this residual part an order parameter S^2 can be calculated. For a rod-shaped molecule with emission moment parallel to the long axis this order parameter is given by

$$S^2 = r(\infty)/r_0 = (\cos\theta_0 (1 + \cos\theta_0)/2)^2 . \tag{11}$$

This describes the equilibrium distribution of the orientations of the absorption and emission dipole moments of the chromophore around its rotational axis in a cone with semiangle θ_0 (Heyn 1979; Lipari and Szabo 1980). Evaluation of $r(\infty)/r_0$ in the case of the yeast $tRNA^{Phe}$-*E. coli* $tRNA_2^{Glu}$ complex yields an angle θ_0 of about 43° for the cone in which wybutine can diffuse freely.

In our model this residual anisotropy part is described by the amplitudes A, B and C, which contain information on the orientation of the wybutine in relation to its rotational axis. An exact analysis of the mean fractional amplitudes of $r(t)$ according to Eq. (8) or a more recent description proposed by Szabo (1984) is beyond the present data statistics.

It is worthwhile pointing out that $r(t)$ at low Mg^{2+} concentration starts at 0.03 and goes through a maximum before decreasing again (Fig. 4A). This property is not observed in the presence of Mg^{2+} and the complementary anticodon. This behaviour can be explained by rotation of wybutine around an axis perpendicular to the base plane, a situation which would occur if wybutine is mobile but in a nucleoside stack.

From r_0 the angle λ between the absorption and emission dipole moment can be calculated from

$$r_0 = (3\cos^2(\lambda) - 1)/5 . \tag{12}$$

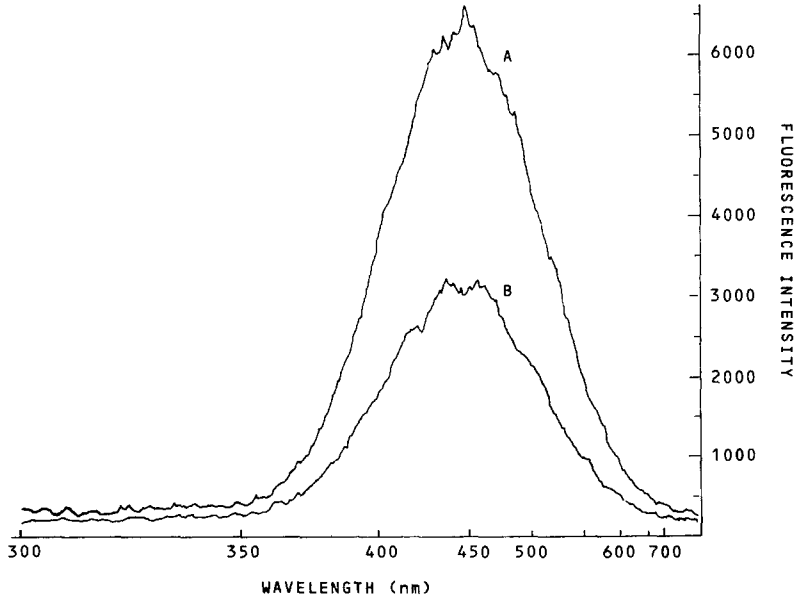

Fig. 6. Time resolved fluorescence spectra of the wybutine in yeast $tRNA^{Phe}$ (*A*) and in the yeast $tRNA^{Phe}$-*E. coli* $tRNA_2^{Glu}$ complex (*B*) at 20 m*M* Mg^{2+} and 20 °C in a time range up to 40 ns

This gives a value for λ of 50° and 52° in the presence and absence of Mg^{2+}, which is the main reason for the low anisotropy value found in stationary measurements (Beardsley et al. 1970; Thiebe and Zachau 1970). In the presence of the *E. coli* $tRNA_2^{Glu}$ anticodon the r_0 value of the fast rotating wybutine has increased to 0.1 (Table 4) which means that the angle λ is reduced significantly. From this behaviour and the fact that $r(t)$ decays in the "normal" way we conclude that the rapid motion of wybutine occurs with less rigid constraints than that observed with the low Mg^{2+}.

Time resolved fluorescence spectra

In order to find out if different lifetimes are related to species with different emission properties time resolved fluorescence spectra were recorded. Spectra of the wybutine in the yeast $tRNA^{Phe}$ molecule alone and in the yeast $tRNA^{Phe}$-*E. coli* $tRNA_2^{Glu}$ complex were taken over the whole time range from 0 to 40 ns (Fig. 6). No apparent differences can be seen. They were also recorded in three different time windows, 0 to 400 ps, 0.5 to 3 ns and 3 to 40 ns. The spectra looked identical to those in Fig. 6 and no significant differences for the various time intervals could be detected (not shown).

Discussion

The fluorescence properties of a natural fluorophore, wybutine, which is situated in the anticodon loop of yeast $tRNA^{Phe}$, adjacent to the three anticodon bases GmAA, were examined in order to obtain information about the existence of different structures of the anticodon loop. From the results it is evident that those properties are different at low Mg^{2+}, high Mg^{2+} concentration or when a "codon" binds to the anticodon.

Structural interpretation, conformations of the anticodon loop

Role of magnesium ions. From the occurrence of three distinct lifetimes (Table 2) of wybutine and the Mg^{2+} dependence of their weighting factors (Fig. 1) we conclude that wybutine senses three different conformations of the anticodon loop. In one wybutine occurs in a longlived fluorescence state (6 ns) and is immobile. In another state wybutine is shortlived and mobile as can be deduced from the anisotropy decay. Since there is no absorption of nucleic acids in the range where wybutine emits, energy transfer as a reason for short lifetimes is unlikely. We favour a model where wybutine looses its fluorescence through dynamic quenching with its environment. The fact that three different conformations exist is in accordance with previous measurements where ethidium, substituted at positions 16/17 and 37, served as a fluorescent probe (Ehrenberg et al. 1979). Temperature-jump experiments, carried out on yeast $tRNA^{Phe}$, monitoring the wybutine fluorescence yield two relaxation processes with relaxation times of the order of 100 µs and 1 ms thus supporting the existence of at least three conformations (Urbanke and Maass 1978; Labuda and Pörschke 1982). Since the fluorescence lifetimes are much shorter than the chemical relaxation times we observe individual conformational states and simultaneously obtain more direct information about their quantum yields. From our measurements it is clear that Mg^{2+} ions shift the equilibrium distribution of conformations towards a state in which the wybutine is fixed and has a long lifetime (6 ns).

It is known that Mg^{2+} ions stabilize the tertiary structure of tRNA. It is evident from the Mg^{2+} dependence of the binding constants (Table 1) that they play an important role in the codon-anticodon interaction. The effect of Mg^{2+} ions on the fluorescence of the wybutine in the yeast $tRNA^{Phe}$ molecule can be explained by the fact that a specific binding site for a Mg^{2+} ion is located in the anticodon loop (Teeter et al. 1980). This Mg^{2+} ion has contact with one phosphate group, in this case P37 attached to the wybutine nucleoside, and has further contacts with base atoms via water molecules. In the latter kind of interaction the N1 of wybutine is involved. Thus it is likely that at high Mg^{2+} concentration this Mg^{2+} ion in the anticodon loop keeps the wybutine in a fixed position, while at low Mg^{2+} concentration wybutine rotates within the nucleoside stack. X-ray analysis shows that the anticodon loop favours the 3′–5′ stack because of the contacts of the hydrated Mg^{2+} ion to various bases, forming an inner sphere complex (Labuda and Pörschke 1982).

Codon-anticodon interaction. Binding the codon s^2UUC of *E. coli* $tRNA_2^{Glu}$ at high Mg^{2+} concentration results in a complete change of the states of wybutine. Two new conformations appear, specified by 0.1 ns and 1 ns, while the 6 ns state of unbound yeast $tRNA^{Phe}$ can still be found. Also in this case high rotational mobility is linked to a state with a short fluorescence lifetime. The rotational motion of wybutine in this conformation shows practically no activation barriers (of order kT) and is of diffusional origin (Table 5).

The fact that the wybutine becomes mobile, but in another way than with low Mg^{2+}, suggests the existence of a conformation different from that in the 3′–5′ stack where the anticodon is basepaired. ^{31}P-NMR studies of yeast $tRNA^{Phe}$ indicate that

upon complexation with the oligonucleotides UUCA and UUCAG the structure of the anticodon loop changes (Geerdes et al. 1980a). In the case of UUCAG, formation of two additional hydrogen bonds on the 5′ side of the anticodon was observed and it was concluded that the anticodon loop can exist in a (5′−3′)-stacked conformation.

The solution structure of a pentadecamer from yeast $tRNA^{Phe}$ consisting of the anticodon stem and loop region, was examined by NMR with and without the codon UpUpC bound to it (Clore et al. 1984). It was found that in this case the pentadecamer adopts a hairpin loop structure with the anticodon loop in the (3′−5′)-stacked conformation in both cases. This result might indicate differences in structural constraints of the anticodon loop stem region when separated from the integral tRNA structure.

From temperature jump experiments with yeast $tRNA^{Phe}$ the coexistence of a (3′−5′)- and (5′−3′)-stacked conformation of the yeast $tRNA^{Phe}$ anticodon loop in solution was proposed (Urbanke and Maass 1978). Additional support for the existence of different anticodon loop conformations stems also from a relaxation kinetic investigation on the $tRNA^{Phe}$-UUC interaction (Labuda and Pörschke 1980). Their result shows preferential interaction of UUC with one anticodon loop conformation followed by a conformational transition of the whole complex.

Chemical relaxation experiments performed with the yeast $tRNA^{Phe}$-*E. coli* $tRNA_2^{Glu}$ complex, in which the fluorescence of the wybutine or of ethidium, substituted at position 16/17 in the *D*-loop, was measured, gave one relaxation time of the order of 100 ms at 20 °C (data not shown). This is in agreement with previous data where the change in absorption of the nucleic acids was measured for the same complex (Grosjean et al. 1976). Our present data unambiguously show that a conformational transition in the anticodon loop of $tRNA^{Phe}$ is involved in the relaxation process. The fact that the wybutine in the anticodon loop and the ethidium in the *D*-loop show exactly the same kinetic behaviour suggests moreover that they witness an overall conformational change taking place in the tRNA upon coding the anticodon.

This idea is supported by several other experiments. Small angle X-ray scattering studies suggest that in the yeast $tRNA^{Phe}$-*E. coli* $tRNA_2^{Glu}$ complex the acceptor and the anticodon arms of the tRNA's are folded towards each other (Nilsson et al. 1982). Support for the possibility of an overall bending motion of the tRNA structure is given by molecular mechanics calculations on yeast $tRNA^{Phe}$ (Harvey and McCammon 1981; Tung et al. 1984). It was found that straightening the tRNA into a nearly linear conformation costs 52 kcal/mole, while bending the acceptor arm −72° towards the anticodon arm needs 94 kcal/mole. In both cases the energy required for those motions is of the same order of magnitude as the change in solvation energy which is due to the change in the surface exposure. This means that those motions can occur spontaneously in solution.

Our data clearly show that the anticodon loop of yeast $tRNA^{Phe}$ undergoes a conformational change on binding a complementary codon triplet. This in turn is likely to trigger an overall change of the whole tRNA molecule. A transition of the anticodon loop from a 3′−5′ stack to a 5′−3′ stack has been proposed by several groups, particularly as a mechanism for the translation process (Crick et al. 1976; Lake 1977; Woese 1970). Although our data cannot be taken as a direct support for such a change, they indicate the existence of an anticodon loop conformation where the motion of wybutine is less restricted than in a 3′−5′ stack.

Acknowledgements. We thank R. Jakabffy, B. Larsson and E. Hagman for expert assistance in preparing and testing the tRNA's and Mrs. K. Nilson for helping with the manuscript. This study has been supported by grants from the Swedish Natural Science Research Council, the Karolinska Institute and the K. & A. Wallenberg foundation.

References

Beardsley K, Tao T, Cantor CR (1970) Studies on the conformation of the anticodon loop of $tRNA^{Phe}$. Effect of environment on the fluorescence of the *Y* base. Biochemistry 9:3524−3532

Benesi HA, Hildebrand JH (1949) A spectrophotometric investigation of the interaction of iodine with aromatic hydrocarbons. J Am Chem Soc 71:2703−2707

Clore GM, Gronenborn AM, Piper EA, McLaughlin LW, Graeser E, Boom JH van (1984) The solution structure of a RNA pentadecamer comprising the anticodon loop and stem of yeast $tRNA^{Phe}$. A 500 MHz ^{1}H-NMR study. Biochem J 221:737−751

Crick FH, Brenner S, Klug A, Pieczenik G (1976) A speculation on the origin of protein synthesis. Origins Life 7: 389−397

Cross AJ, Waldeck DH, Fleming GR (1983) Time resolved polarization spectroscopy: Level kinetics and rotational diffusion. J Chem Phys 78:6455−6467

Ehrenberg M, Rigler R, Wintermeyer W (1979) On the structure and conformational dynamics of yeast phenylalanine-accepting transfer ribonucleic acid in solution. Biochemistry 18:4588−4599

Eisinger J (1971) Complex formation between transfer RNA's with complementary anticodons. Biochem Biophys Res Commun 43:854−861

Eisinger J, Feuer B, Yamane T (1970) Luminescence and binding studies on $tRNA^{Phe}$. Proc Natl Acad Sci USA 65:638−644

Geerdes HAM, Boom JH van, Hilbers CW (1980a) Nuclear magnetic resonance studies of codon-anticodon interaction

in $tRNA^{Phe}$. I. Effect of binding complementary tetra and pentanucleotides to the anticodon. J Mol Biol 142: 195–217

Geerdes HAM, Boom JH van, Hilbers CW (1980b) Codon-anticodon interaction in $tRNA^{Phe}$. II. A nuclear magnetic resonance study of the binding of the codon UUC. J Mol Biol 142:219–230

Grinvald A, Steinberg IZ (1974) On the analysis of fluorescence decay kinetics by the method of least-squares. Anal Biochem 59:583–598

Grosjean H, Söll DG, Crothers M (1976) Studies of the complex between transfer RNA's with complementary anticodons. I. Origins of enhanced affinity between complementary triplets. J Mol Biol 103:499–519

Grosjean HJ, De Henau S, Crothers D (1978) On the physical basis for ambiguity in genetic coding interactions. Proc Natl Acad Sci USA 75:610–614

Harvey SC, McCammon JA (1981) Intramolecular flexibility in phenylalanine transfer RNA. Nature 294:286–287

Heyn MP (1979) Determination of lipid order parameters and rotational correlation times from fluorescence depolarization experiments. FEBS Lett 108:359–364

Kim SH, Suddath FL, Quigley GJ, McPherson A, Sussman JL, Wang AHJ, Seeman NC, Rich A (1974) 3-dimensional tertiary structure of yeast phenylalanine transfer-RNA. Science 185:435–440

Labuda D, Pörschke D (1980) Multistep mechanism of codon recognition by transfer ribonucleic acid. Biochemistry 19: 3799–3805

Labuda D, Pörschke D (1982) Magnesium ion inner sphere complex in the anticodon loop of phenylalanine transfer ribonucleic acid. Biochemistry 21:49–53

Ladner JE, Jack A, Robertus JD, Brown RS, Rhodes D, Clark BFC, Klug A (1975) Structure of yeast phenylalanine transfer-RNA at 2.5 Å resolution. Proc Natl Acad Sci USA 72:4414–4418

Lake JA (1977) Aminoacyl-tRNA binding at the recognition site is the first step of the elongation cycle of protein synthesis. Proc Natl Acad Sci USA 74:1903–1907

Lipari G, Szabo A (1980) Effect of librational motion on fluorescence depolarization and nuclear magnetic resonance relaxation in macromolecules and membranes. Biophys J 30:489–506

Marquardt DW (1963) An algorithm for least-squares estimation of non-linear parameters. J Soc Ind Appl Math 11:431–441

Meeter DA (1964) Non-linear least-squares (Gaushaus). University of Wisconsin Computer Center

Nilsson L, Rigler R, Laggner P (1982) Structural variability of tRNA: Small-angle X-ray scattering of the yeast $tRNA^{Phe}$-*Escherichia coli* $tRNA_2^{Glu}$ complex. Proc Natl Acad Sci USA 74:1903–1907

Quigley GJ, Rich A (1982) Cited in Rigler R, Wintermeyer W (1983)

Rigler R, Ehrenberg M (1973) Molecular interactions and structure as analyzed by fluorescence relaxation spectroscopy. Qu Rev Biophys 6:139–199

Rigler R, Ehrenberg M (1976) Fluorescence relaxation spectroscopy in the analysis of macromolecular structure and motion. Qu Rev Biophys 9:1–19

Rigler R, Wintermeyer W (1983) Dynamics of tRNA. Annu Rev Bioeng 12:475–505

Rigler R, Claesens F, Lomakka G (1984) Picosecond single photon counting fluorescence spectroscopy of nucleic acids. In: Auston DH, Eisenthal KB (eds) Ultrafast phenomena IV. Springer, Berlin Heidelberg New York, pp 472–476

Rigler R, Claesens F, Kristensen O (1986) Ultrafast-fluorescence with picosecond lasers and multichannel plate detectors. Anal Instrum 14:525–546

Szabo A (1984) Theory of fluorescence depolarization in macromolecules and membranes. J Chem Phys 81:150–167

Teeter M, Quigley GJ, Rich A (1980) Metal ions and transfer RNA. In: Spiro TG (ed) Nucleic acid-metal ion interactions. Wiley, New York, pp 145–176

Thiebe R, Zachau HG (1970) Further studies on amino acid acceptance and physical properties of yeast $tRNA^{Phe}$. Biochim Biophys Acta 217:294–304

Tung C-S, Harvey SC, McCammon CA (1984) Large-amplitude bending motions in phenylalanine transfer RNA. Biopolymers 23:2173–2193

Urbanke C, Maass G (1978) A novel conformational change of the anticodon region of $tRNA^{Phe}$ (yeast). Nucleic Acids Res 5:1551–1560

Woese C (1970) Molecular mechanics of translation: a reciprocating ratchet mechanism. Nature 226:817–820

Yoon K, Turner DH, Tinoco I Jr (1975) The kinetics of codon-anticodon interaction in yeast phenylalanine transfer RNA. J Mol Biol 99:507–518